PROCEEDINGS OF SCIENCE

Directional Visualization of Space Radiation Quanta with Timepix/SATRAM Spacecraft Payload on board ESA Proba-V Satellite

Carlos Granja[1], **Stepan Polansky, Stanislav Pospisil, Daniel Turecek, Zdenek Vykydal**
Institute of Experimental and Applied Physics (IEAP), Czech Technical University in Prague (CTU)
Horska 3a/22, 128 00 Prague 2, Czech Republic
E-mail: carlos.granja@utef.cvut.cz

Alan Owens, Karim Mellab, Petteri Nieminen
European Space Research & Technology Centre (ESTEC), European Space Agency (ESA)
Postbus 299, NL-2200 AG Noordwijk, The Netherlands

Zdenek Dvorak, Marek Simcak, Zdenek Kozacek, Petr Vana, Jan Mares
Czech Space Research Center (CSRC)
Janska 12, 602 00 Brno, Czech Republic

The compact light weight SATRAM payload, which is based on the hybrid semiconductor pixel detector Timepix, is operating in open space onboard ESA's Proba-V satellite in low Earth orbit since 7th May 2013. The Timepix chip can determine the composition and spectral characteristics of ionizing radiation in the satellite environment. The device provides single quantum X-ray photon and charged particle counting for high sensitivity detection, high resolution tracking and directional visualization of energetic charged particles over a wide dynamic range of particle fluxes, energies and broad field of view. The motivation for this work and short description of the detector is given together with first results of its response in open space. Preliminary results on particle/dose rate in spatial and time correlated maps along the satellite orbit are presented.

X Latin American Symposium on Nuclear Physics and Applications (X LASNPA)
1-6 December 2013
Montevideo, Uruguay

[1] Speaker

PoS(X LASNPA)003

1. Introduction

The Space Application of Timepix Radiation Monitor (SATRAM) is a compact low-mass and low-power spacecraft payload operating in open space on board in the ESA's Proba-V satellite [1]. Launched on 7th May 2013, the satellite is deployed in Low Earth Orbit (LEO) at an altitude 820 km. The satellite operates (LEO) at altitude 820 km. SATRAM provides high-sensitivity wide-dynamic range radiation monitoring enhanced with particle track visualization of the charged events and low-energy X-ray field along the satellite orbit. The Timepix detector [2] determines over a wide range of particle fluxes, energies and broad field of view [3] the composition and spectral characterization of the mixed field radiation environment [4]. The per-pixel energy sensitivity provides linear energy transfer (LET) spectra with enhanced particle-type resolving power and directional sensitivity for energetic charged particles. Results can include spatial- and time-dependent distributions of the radiation environment along the satellite orbit as presented in this contribution.

The range of applications of the Timepix detector [3] includes aircraft atmospheric [5] and balloon-borne stratospheric [6] cosmic-ray detection as well as space-crew radiation dosimetry at low Earth orbit (LEO) on-board the International Space Station inside an air pressurized NASA ISS module [7-8]. On the other hand, in open space, developments so far exist for other technologies such as the semiconductor diode Standard Radiation Environment Monitor [9] and the Energetic Particle Telescope [10].

1.1 Near Earth radiation environment and spacecraft onboard radiation monitoring

Radiation environment monitoring has become an essential component of the space segment of any mission, having impact, not only on spacecraft operations but also on future missions and operations. Precise measurement and high sensitivity monitoring of the radiation field onboard satellites in near Earth orbit are necessary for detailed assessment of radiation effects on spacecraft components and electronic devices – e.g. [11], space radiation environment and space weather physics studies [12-13]. Time- and spatially-correlated measurements serve for studies of variations energetic radiation such as the highly variable solar particle events (SPE) and coronal mass ejections [14], the trapped radiation and dynamics of the Earth radiation belts. Experimental data serve as direct input for systematic studies of space weather and atmospheric radiation physics, dosimetric data surveys and space radiation compilations, the Earth magnetosphere and near-Earth radiation belt models [15-16] as well as reference and verification for model-based and Monte-Carlo calculations of radiation transport and shielding – e.g. [17].

The near Earth radiation environment is highly dynamic and complex in terms of composition, energies, fluxes and directional distribution [18-19]. The main source components of the radiation environment at LEO are the trapped radiation in the Earth radiation belts, SPEs and galactic cosmic rays. The mixed radiation field consists of X- and gamma-rays, light and heavy charged particles such as electrons, protons, light and heavy ions as well as neutrons in very wide ranges of energy and flux. The LEO radiation intensity is highly variable in time (e.g.

during SPEs) but also in position (latitude, longitude) [18-19] along the given satellite orbit and altitude – e.g. [20].

2. The Timepix hybrid semiconductor pixel detector

The position-sensitive semiconductor detectors of the Medipix family [2,21], developed in frame of the MEDIPIX Collaboration provide high sensitivity (single-particle/quantum counting), wide-dynamic range, high spatial resolution and noiseless (dark-current free) detection. The hybrid architecture enables using sensors of defined media (e.g., Si, CdTe, GaAs) and thicknesses (e.g., 300 um, 700 um, 1000 and 1500 um). The detector consists of a matrix of 256 × 256 (total of 65.536) pixels, pixel pitch size 55 μm and full sensitive area 14 mm × 14 mm (1.98 cm^2) – see Fig. 1.

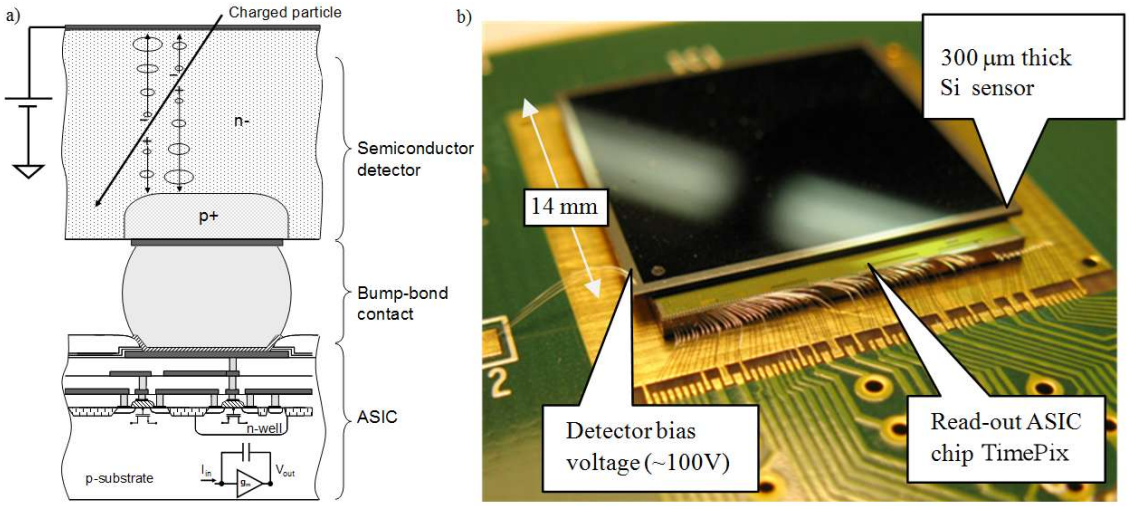

Fig. 1: (a) Illustration at the pixel scale (pixel pitch size 55 μm) of (b) the Timepix detector consisting of a semiconductor sensor (of size 14 mm × 14 mm and thickness 300 μm) bump bonded to the integrated ASIC readout chip of 256 × 256 pixels (total 65.356 channels).

Based on the Medipix2 [21] device, Timepix [2] provides extended functionality at the level of the per-pixel integrated electronic chain. Each pixel of the Timepix detector can be independently configured to operate in *counting mode* (the counter is incremented by one when the per-pixel deposited energy of the interacting particle crosses a threshold level), *energy mode* (called Time-over-Threshold (ToT) mode where the counter is incremented continuously as long as the signal is above threshold) and *Time mode* (called Time-of-Arrival (ToA) mode where the counter is incremented continuously from the time the first hit arrives until the closure of the shutter or end of the time window or acquisition exposure). Equipped with a 300 μm thick silicon sensor, Timepix is sensitive to X-rays (highest efficiency in the range 5–25 keV) and charged particles (100% detection efficiency) with a detection threshold of 4 keV.

3. Timepix/SATRAM spacecraft payload

The Space Application of Timepix based Radiation Monitor (SATRAM) is a technology demonstration payload as a spacecraft platform device on-board ESA's Proba V satellite which was launch on 7th May 2013. The payload contains an FPGA controlling the Timepix detector and provides communication with the spacecraft, along with housekeeping, data compression and configuration. Including the Aluminum alloy compartment the payload has dimensions 108 mm × 63 mm × 56 mm (see Fig. 2), a full volume of 380 ml and a total weight of 172 g. The entrance window in front of the Timepix chip is of 0.5 mm thick Al. The payload features 28 V voltage input and power consumption ≤ 3 W.

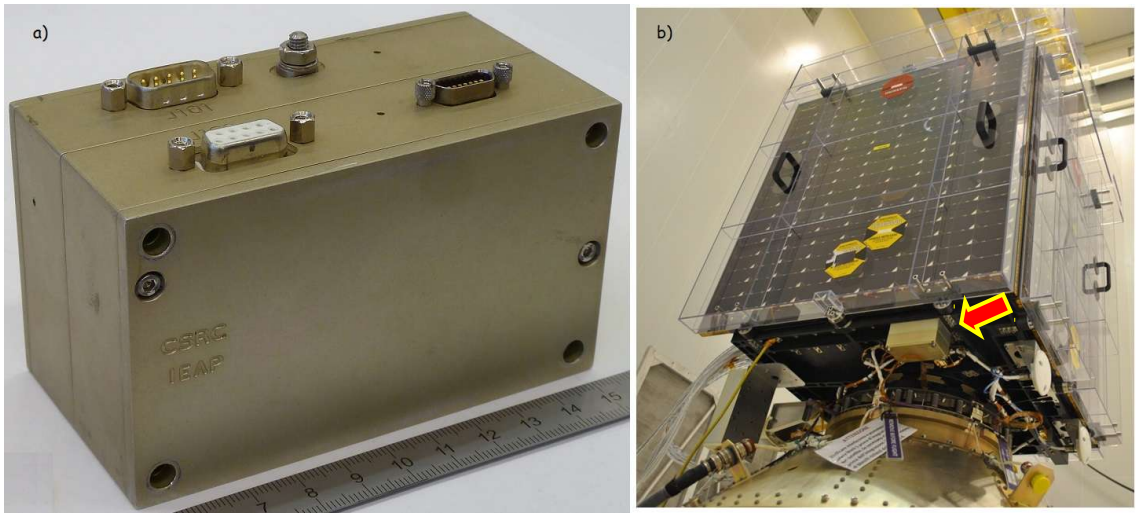

Fig. 2: SATRAM payload (a) attached on the exterior of ESA's Proba-V satellite (b) prior launch by ESA's Vega-2 rocket. Proba-V satellite size: 80 cm × 80 cm × 100 cm and mass: 138 kg. The plastic side panels with handles are protective covers which were removed before flight.

Energy calibration of the Timepix detector was performed with X-ray and alpha particle radioactive sources. Test and response characterization were done also with a radionuclide neutron source (AmBe) and low-energy light ion (proton, deuterium and alpha particle) beams and mono-energetic fast neutron sources from the Van de Graaff accelerator at the IEAP CTU in Prague.

3.1 Configuration and operation of the Timepix/SATRAM payload

The operation of the Timepix detector requires setting several parameters including the sensor bias (range 0 to + 100 V), frame exposure time (arbitrary values can be set in the range from µs thru ms up to s and longer), high frequency clock (set at 11.059 MHz), pixel mode mask (each pixel can be independently set to energy (ToT), time (ToA) or counting (MPX) mode), masked pixel matrix (switching off noisy pixels), and the per-pixel DAC parameters such as pulse shaping IKRUM, threshold THL, baseline FBK parameters (in total fourteen DACs). These detector operation values are stored at by the satellite and can be modified by telecommand data packet uplink.

4. Detection and track visualization of space radiation in open space in LEO orbit

The detection of space radiation is shown in Fig. 3. Single particles are detected and their tracks in the pixelated matrix are visualized at the pixel-size scale. Energetic heavy and light charged particles produce tracks involving many pixels of characteristic morphology [4].

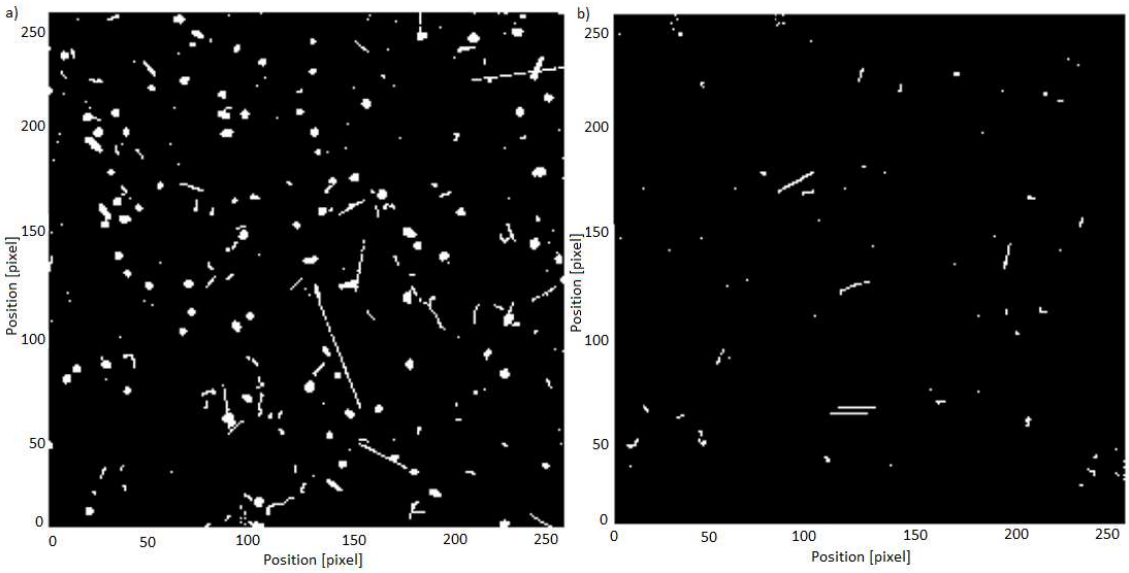

Fig. 3: Quantum imaging detection of space radiation by Timepix/SATRAM payload in open space along ESA's Proba-V satellite LEO orbit (820 km altitude): region of high (a) and low (b) radiation. Data displayed in counting mode, 5 s acquisition time. The whole sensor matrix (256×256 pixels) is displayed (14 mm×14 mm = 1.98 cm^2).

The spatial resolution of the Timepix chip ranges from the level of the pixel size (55 μm) down to few μm [22-23] and can be even higher (sub μm) [24]. In addition to the morphology information of the particle tracks (Fig. 3), the per-pixel energy sensitivity of Timepix enables measuring the energy deposited by the particle in the sensor (see Fig. 4). The energy deposited is given by the sum of the responses in all pixels registered in the particle signal (forming a *cluster* of pixels). The energy resolution is 100 keV FWHM for 5.5 MeV alpha particles.

4.1 Particle type resolving power & particle flux

Single particles produce in the pixelated detector clusters of different deposited energy, varying size (number of pixels) and shape (round, elongated, short and long or narrow and broad tracks) which are analyzed in order to obtain information about the particle type, deposited energy, and direction. Event-by-event analysis of single particle tracks by pattern recognition algorithms is used for resolving the particle type according to characteristic morphology patterns and energy loss – see Fig. 4. Light charged particles produce characteristic small and narrow tracks. Heavy charged particles produce characteristic large and broad tracks. For energetic charged particles and minimum ionizing particles the track length, particle direction (see Sec. 4.2) and linear energy transfer can be derived. The number of counted and/or selected particles over unit area and time interval can provide particle-type particle flux.

4.2 Directional sensitivity & wide field of view

For energetic charged particles, information on the particle's direction of trajectory can be derived. The relative direction of incidence of the particle trajectory onto the sensor plane can be provided in 3D. Two angle components can be expressed: elevation angle (from the sensor plane) and projection angle (along the sensor plane). The angular resolution varies from few tens of degrees (perpendicular direction of incidence) down to few degrees (grazing angles) [24] and even sub-degree resolution (parallel direction of incidence). A wide field of view (2π) can be covered, with additional information also present on the penetrating and secondary particles from the spacecraft.

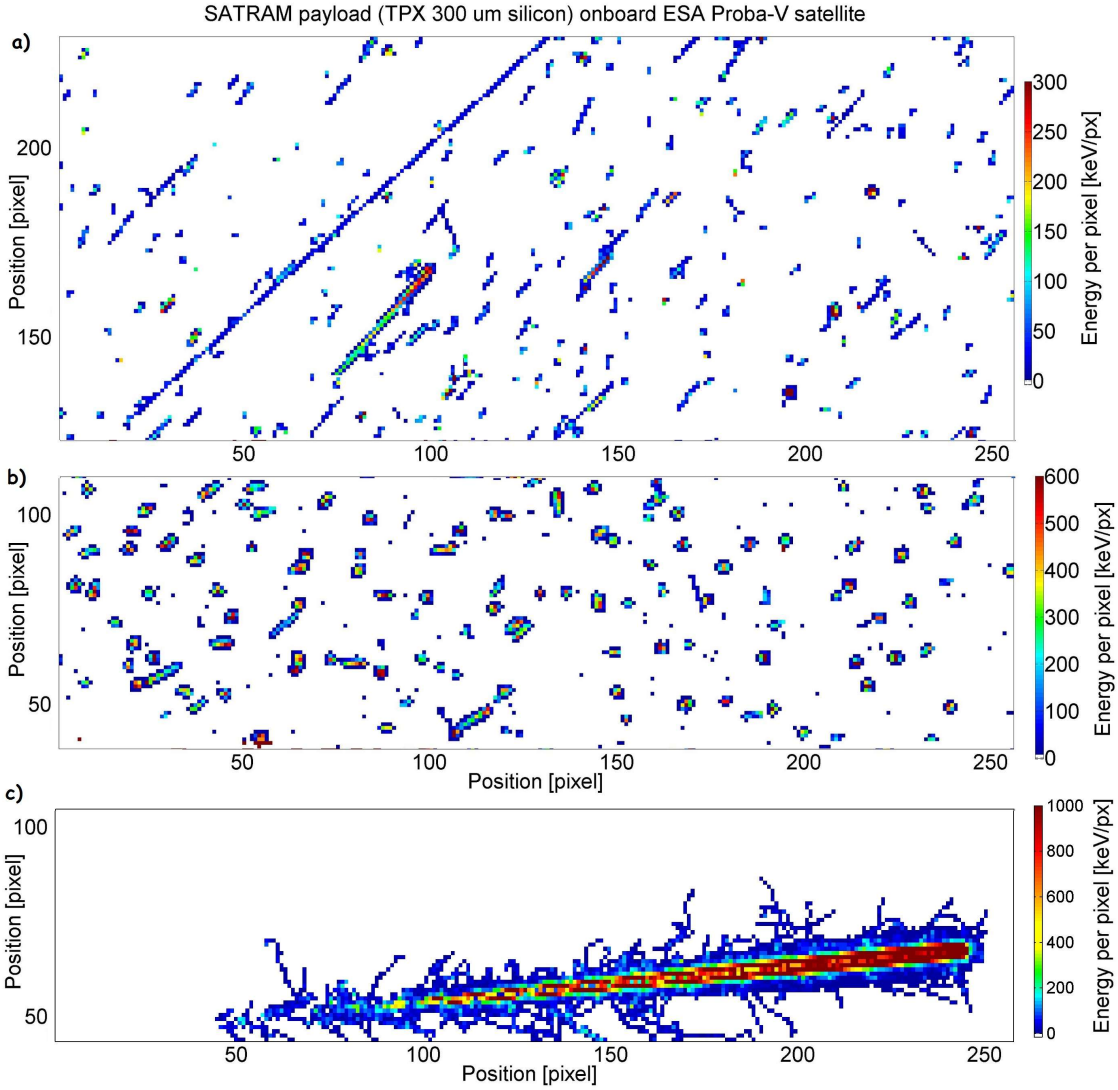

Fig. 4: Similar as Fig. 3 displaying radiation from regions with a dominant component of highly directional field of mostly (a) light and (b) heavy charged particles. The track of a single (c) high-Z highly energetic heavy particle with associated delta electrons is included. Data displayed in Timepix energy/ToT mode where the per-pixel energy response is shown in color (displayed in different scale for each plot). Only parts of the sensor pixel matrix are displayed.

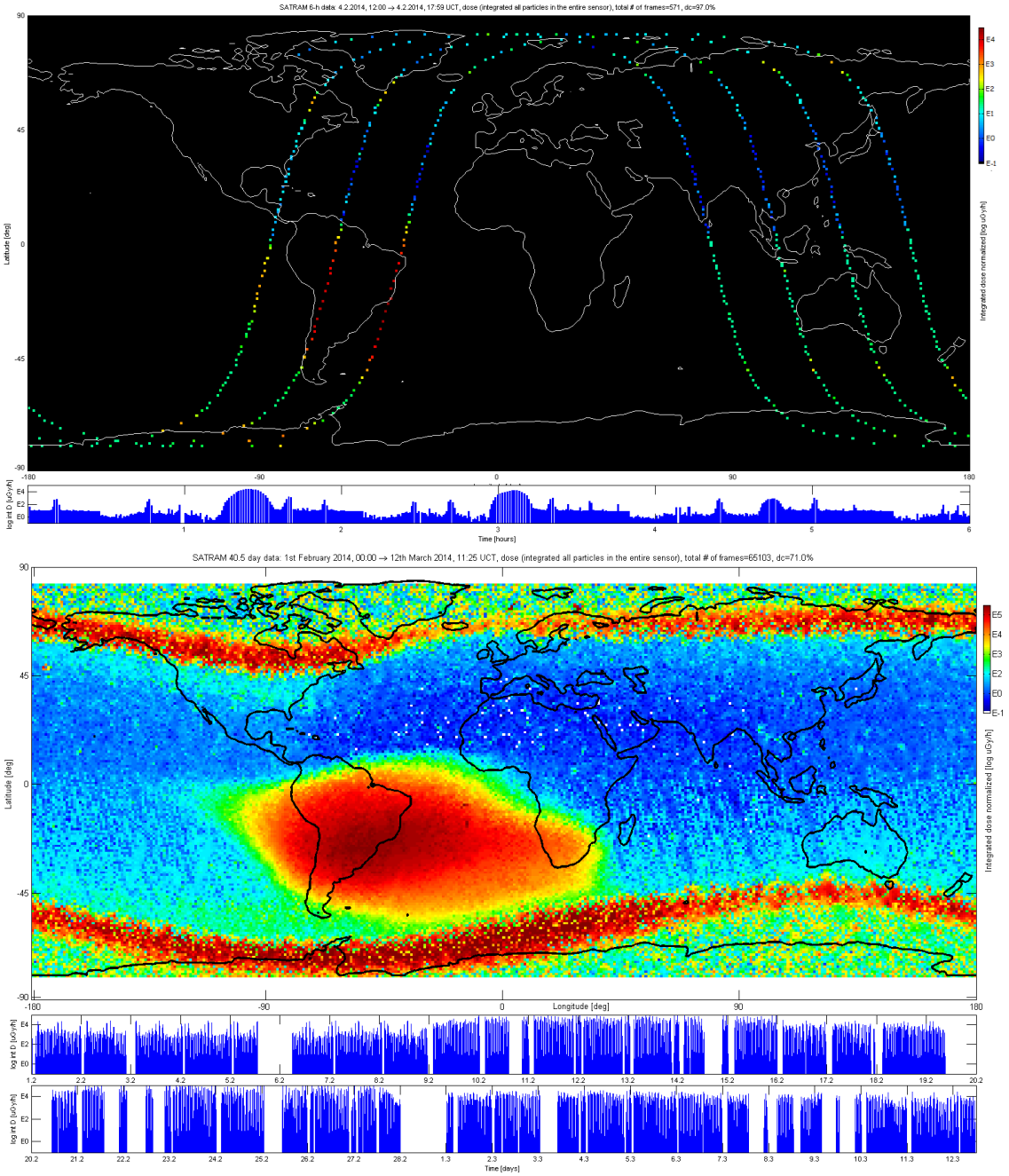

Fig. 5: Spatial and time distributions of total absorbed dose at 820 km LEO orbit measured by SATRAM. Results are shown for 6 h (top) and 40 day (bottom) periods (on 4th February 2014 and during 1st February thru 13th March 2014, respectively). Data from a total of 571 and 65.103 Timepix frames collected over these periods, respectively (overall SATRAM operation duty cycle 97% and 71%, respectively). The quantity displayed (total absorbed dose, displayed in uGy/h) spans over 6 orders of magnitude (see color bar log scale).

5. Spatial and time distributions of radiation dose along the satellite orbit

SATRAM can sample the radiation field along the satellite path (sun synchronous polar orbit tilted at 98.8º) and altitude (820 km). The spatial and time maps of the total absorbed dose measured by SATRAM in a 6 hours and 40 days are given in Fig. 5.

The correlated time distributions are included below each spatial plot displaying the evaluated quantity (total absorbed dose) along the selected period. The spatial map displayed in more detail in perspective globe view is shown in Fig. 6. The empty intervals indicate periods when SATRAM was not in operation. The vertical axis is given in logarithmic scale.

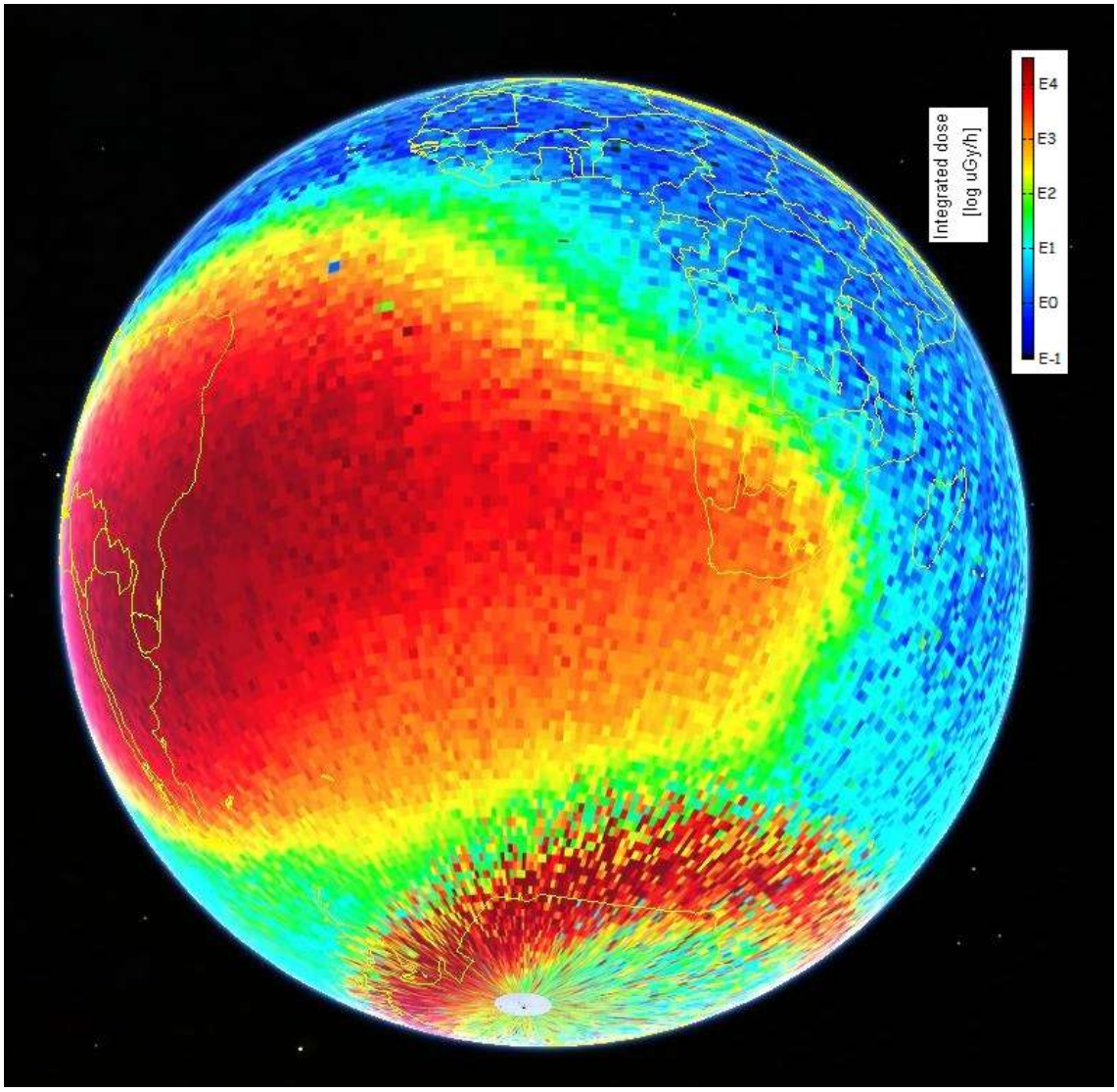

Fig. 6: Similar to Fig. 5 showing the Earth map of total absorbed dose displayed in perspective view over the region above the South Atlantic and the South Pole. Data from 104.316 Timepix frames acquired for a period of 66 days from 1st January thru 7th March 2014 (overall SATRAM operation duty cycle 68%).

6. Conclusions

SATRAM is the first deployment of the Timepix detector in open space. The payload has been successfully commissioned. The detector configuration and measurement settings such as the detector acquisition time are being refined for appropriate performance in terms of event cluster occupancy, payload operation duty-cycle, on-board memory capacity and downlink transfer rate. Detailed data analysis is in progress. Data evaluation including results according particle type is underway. Future work includes refinement and further development of SATRAM operation to allow for reconstruction of the environmental charged particle flux and radiation component and spectral characterization.

Acknowledgments

Research performed in frame of the IEAP CTU and Medipix Collaboration. Project funded by the European Space Agency, Grant No. 4000105089/11/NL/CBi (641-120004M). Calibration and testing measurements of the Timepix detector performed at the Van de Graaff light ion accelerator of the IEAP CTU in Prague were supported by the Grant Research Infrastructure No. LM2011030/149-120006M of the Ministry of Education, Youth and Sports of the Czech Republic.

References

[1] B. Sean, *The mission of Proba-V*, ESA Bulletin, European Space Agency 153 (2013) 10-21 (see http://esamultimedia.esa.int/docs/Proba/Bulletin_Proba-v.pdf).

[2] X. Llopart, M. Campbell, E. Heijne, et al., *Timepix, a 65 k programmable pixel readout chip foarrival time, energy and/or photon counting measurements*, Nucl. Instr. and Meth. in Phys. Res. A 581 (2007) 485-494.

[3] E.H.M. Heijne, R. Ballabriga, M. Campbell, et al. *Measuring radiation environment in LHC or anywhere else, on your computer screen with Medipix*, Nucl. Instr. and Methods A 699 (2013) 198-204.

[4] Z. Vykydal, J. Bouchami, M. Campbell, et al., *The Medipix2-based network for measurement of spectral characteristics and composition of radiation in ATLAS detector*, Nucl. Instr. Meth. Phys. Res. A 607 (2009) 35-37.

[5] C. Granja, S. Pospisil, *Quantum imaging dosimetry and online visualization of X-ray and charged-particle radiation inside aircraft at aviation altitudes with the pixel detector Timepix*, Adv. Space Res. 54 (2014) 241-251.

[6] J. Urbar, J. Scheirich, J. Jakubek, *Medipix/Timepix cosmic ray tracking on BEXUS stratospheric balloon flights*, Nucl. Instr. and Meth. in Phys. Res. A 633 (2011) S206-S209.

[7] Turecek, D., Pinsky, L., Jakubek, J., Vykydal, Z., Stoffle, N., S Pospisil, S., *Small Dosimeter based on Timepix device for International Space Station*, J. of Instrumentation 6 (2011) C12037.

[8] Pinsky, L., N. Stoffle, J. Jakubek, et al., *Application of the Medipix-2 technology to space radiation dosimetry and hadron therapy monitoring*, Nucl. Instr. and Meth. in Phys. Res. A 628 (2011) 226-229.

[9] H.D.R. Evans, P. Buhler, W. Hajdas, E.J. Daly a, P. Nieminen a, A. Mohammadzadeh, *Results from the ESA SREM monitors and comparison with existing radiation belts*, Adv. Space Res. 42 (2008) 1527-1537.

[10] M. Cyamukungu, G. Gregoire, The Energetic Particle Telescope (EPT) concept and performances, Proc. SPIE 8148, Solar Physics and Space Weather Instrumentation IV, 814803 (2011).

[11] M.W. Shin, Kim, M.-H. An evaluation of radiation damage to solid state components flown in low earth orbit satellites. Rad. Prot. Dosimetry 108 (2004) 279-291.

[12] H. Koshiishi, H. Matsumoto, *Space radiation environment in low earth orbit during solar-activity minimum period from 2006 through 2011*, J. Atm. and Solar-Terr. Physics 99 (2013) 129-133.

[13] G. Santin, H. Evans, R. Lindberg, P. Nieminen, A. Mohammadzadeh, E. Daly, *Monitoring and simulation of the radiation environment for manned and unmanned space missions*, Nucl. Phys. B 172 (2007) 321-323.

[14] H. Mavromichalaki, G. Souvatzoglou, C. Sarlanis, et al., *Space weather prediction by cosmic rays*, Adv. Space Res. 37 (2006) 1141-1147.

[15] G. D. Reeves, et al. *Electron acceleration in the heart of the Van Allen radiation belts*, Science 341 (2013) 991-994.

[16] M.A. Xapsos, P.M. O'Neill, T.P. O'Brien, *Near-Earth space radiation models*, IEEE Trans. Nucl. Sci. 60 (2013) 1691-1705.

[17] Z.W. Lin, J.H. Adams, A.F. Barghouty, et al. *Comparisons of several transport models in their predictions in typical space radiation environments*, Adv. Space Res. 49 (2012) 797-806.

[18] K. Kudela, *On energetic particles in space*, Acta Physica Slovaca 59, 5 (2009) 537-652.

[19] S. Bourdarie, M. Xapsos, *The near Earth space radiation environment*, IEEE Trans. Nucl. Sci. 55 (2008) 1810-1832.

[20] H. Koshiishi, *Space radiation environment in low earth orbit during influences from solar and geomagnetic events in December 2006*, Adv. Space Res. 53 (2014) 233-236.

[21] X. Llopart, M. Campbell, R. Dinapoli, et al., *Medipix2: a 65-k pixel readout chip with 55 um square elements working in single photon counting mode*, IEEE Trans. Nucl. Sci. 49 (2002) 2279-2283.

[22] C. Granja, J. Jakubek, U. Koester, M. Platkevic, S. Pospisil, *Response of the pixel detector Timepix to heavy ions*, Nucl. Instr. Methods A 633 (2011) S198-S202.

[23] C. Granja, P. Krist, D. Chvatil, J. Solc, S. Pospisil, J. Jakubek, L. Opalka, *Energy loss and online directional track visualization of fast electrons with the pixel detector Timepix*, Rad. Measurements 59 (2013) 245-261.

[24] E.H.M. Heijne, R. Ballabriga, D. Boltje, et al., *Vectors and submicron precision: redundancy and 3D stacking in silicon pixel detectors*, J. of Instrumentation JINST 5 (2010) C06004.